J Mol Model (2013) 19:631–646
DOI 10.1007/s00894-012-1585-y

ORIGINAL PAPER

Proton affinity of para-substituted acetophenones in gas phase and in solution: a theoretical study

Abir Haloui · Ezzeddine Haloui

Received: 28 March 2012 / Accepted: 28 August 2012 / Published online: 21 September 2012

Abstract The gas phase proton affinities PA and basicities GB for a series of para-substituted acetophenones weak bases (B) p.X−C_6H_4CO*CH_3 with X=H, F, Cl, Br, I, Me, CF_3, CN, NO_2, OCH_3, NH_2, CH_2OH, N$(CH_3)_2$, OH, NH_3^+, … have been calculated at 298.15 K at the density functional theory DFT/B3LYP level with a 6-311++G (2d,2p) basis set. Conformational results lead to only one stable planar conformer for both unprotonated compounds and their O*-protonated forms. Satisfactory accuracy and computational efficiency could be reached if the computed PAs are scaled by a factor 0.983. Protonation at more than one site is discussed and the carbonyl oxygen atom is found to be the preferential protonated site rather than the substituent X. The calculated gas phase PAs show a good agreement with the experimental available data. The electron-donating/electron-withdrawing nature of the substituents has an enormous influence upon the thermochemical and structural properties. The influence of environment on the proton affinity has been studied by means of SCRF solvent effect computations using PCM solvation model for two solvents: water and SO_2CI_2. Confrontation between computed and experimental pK(B) values exhibits better agreement in aqueous solution than in organic solvent.

Keywords DFT(B3LYP) · Para-substituted acetophenones · pK_b · Proton affinity · Solvent effect · Substituent effect

A. Haloui (✉) · E. Haloui
Department of Chemistry, Faculty of Sciences,
Manar 2,
2092 Tunis, Tunisia
e-mail: abirhaloui83@yahoo.fr

Introduction

Over the last three decades, protonation reactions have been the subject of extensive investigations in physical organic chemistry and biochemistry from both an experimental and theoretical point of view [1–22]. Protonation consists of the addition of a proton H^+ to an atom, molecule or ion. The proton affinity (PA) and the gas-phase basicity (GB) are the two most pivotal quantities used to understand the proton transfer process and are directly related to the acid–base approach [2–4, 22–25]. A great number of experimental studies have measured the basicities of organic compounds in both gas phase and solution-phase using modern mass spectrometric techniques. Measurements were performed by spectroscopic methods in acid media [9–14, 16], kinetic method with a tandem mass spectrometer [17], Fourier transform ion cyclotron resonance (FT-ICR) mass spectrometry [17, 23, 26], etc. Despite these numerous experimental studies, a detailed characterization of structural and thermochemical parameters is still largely unknown, especially in solution. In the last few years, several experimental studies have been combined with theoretical approaches to provide a full partnership with experiment. Ab initio (HF, MPn [4, 6, 27–34] and G3 [23, 26, 35–37]) as well as semi empirical quantum methods [5] were used to get energetic data. Deakyne summarized the performances for the most important theoretical methods [25]. As for DFT methods, they have been tested with various functionals by evaluating the proton affinities of bio-molecules and small molecular systems [4, 20, 24, 30–33, 38–44]. It is now well established that modern DFT functionals are good candidates to provide reliable results of thermodynamic properties. Pokon et al. [37] showed that hybrid DFT methods for small molecular systems are much cheaper and competitive with G2 and G3

theories. It should be interesting to confirm this advantageous feature by investigating larger molecular systems.

Substituent effects on acid–base behavior have been a matter of debate in the last years. They were largely considered in both experimental and theoretical studies as one of the most important factors to determine molecular basicity [15–17, 20, 25, 27, 34, 42–44]. Deakyne gathered in reference [25] the different models to probe substituent effects. The presence of the substituent on the aromatic ring, not necessarily a phenyl ring, was the subject of extensive works [15–17, 27, 28, 41]. Kukol et al. summarized in their introduction the essential of studies dealing with ortho-, meta- and para- position effects on aromatic carbonyl compounds [17]. Substituent effects were subdivided into polar and steric effects. Other studies were concerned with the additivity of substituent effects when two or more substituents are present on the aromatic cycle [15, 17, 27, 28]. In general, polar effects were rather discussed in term of strong resonance interaction with electron-donating/withdrawing character of the substituent [15, 17].

Problems concerning phenomena occurring in solution are of interest in many fields of chemistry and biochemistry. Computational chemistry has known the move from the study of isolated molecules to that of solutions which is considered as one of the most important developments in theoretical chemistry [45–47]. A number of papers have been published dealing with the influence of solvent on the thermochemical behavior [32, 34, 39, 40]. The self consistent reaction field SCRF continuum solvation method has been widely adopted in the description of solute-solvent interactions [32, 39, 40]. The PCM method in particular has achieved a considerable degree of success in the calculation of thermochemical properties [40]. Among previous studies concerning protonation in solution, solute-solvent interactions were discussed and related essentially to the polarity of the medium [39, 40].

The purpose of this work is to theoretically investigate the gas-phase proton affinities of a series of para substituted acetophenones p.X−$C_6H_4CO^*CH_3$ containing electron-withdrawing or electron-releasing substituents X (see Fig. 1 for molecule schemes and numbering of atoms). As a matter of fact, the unity C_6H_4-CO always deserves attention owing to the fact that it is often incorporated in interesting large molecular systems (bio-molecules, polymers, …). Also, this paper aims to demonstrate that obtaining accurate and satisfactory values for proton affinities does not necessarily need computationally very expensive models, which could accommodate many users. Calculations were carried out on the neutral and protonated compounds. Computed PAs values were compared with available experimental reference values for the majority of compounds from NIST Database [48]. A number of computed parameters such as the net charge on the particular atoms, bond lengths of both unprotonated and their O*-protonated counterparts has been correlated with computed PAs. In this paper, we also discuss the change in the proton affinities when going from the electron-withdrawing to electron-releasing substituents. In the last part of this work, we look into the SCRF solvent effects using the PCM model and performing calculations for two solvents with quite different dielectric constants (ε=9.15 and ε=78.80).

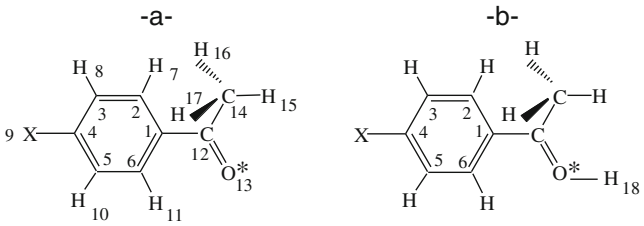

Fig. 1 Numbering of atoms in the considered compounds -**a**- unprotonated form, -**b**- protonated form

Computational procedures

Quantum mechanical calculations of all structural and thermodynamic properties were performed using the program Gaussian03 package [49]. Density functional theory DFT approach with the B3LYP functional and 6-311++G(2d,2p) basis set was applied, except in the case of the iodine derivative for which a limited number of basis sets is available in the standard Gaussian03 software; the corresponding structure was optimized with the aug-cc-pVQZ-PP basis set taken from reference [50]. The choice of this level of theory is justified from our previous work [51] and reference [31]. All optimized structures were subjected to vibrational frequency analysis to verify that the geometries were minima on the potential energy surface. The electron densities were calculated according to Mulliken and Breneman-Wiberg net charge population analysis. We have additionally carried out calculations in solution using the integral equation formalism polarizable continuum model (IEF-PCM) in which the solvent is represented by an infinite dielectric medium.

The gas-phase proton affinity PA and gas-phase basicity GB of a compound B are defined as negative of the change in molar enthalpy and molar free enthalpy at 298.15 K, respectively associated with the gaseous reaction (1) :

$$B(g) + H^+(g) \quad \rightarrow \quad BH^+(g) \quad \begin{cases} \Delta_{prot}\mathrm{H} \equiv -PA \\ \Delta_{prot}\mathrm{G} \equiv -GB \end{cases}, \qquad (1)$$

B and BH^+ denote the unprotonated (base) and the protonated (conjugated acid) forms, respectively.

The gas-phase PA of a molecule A is determined according to Eq. 2:

$$PA = -\left[\Delta E_{el} + \Delta ZPVE + \Delta E_{vib} - \frac{5}{2}RT\right], \quad (2)$$

where ΔE_{el}, $\Delta ZPVE$ and ΔE_{vib} correspond to the differences between total electronic energy, zero-point vibrational energy and temperature-dependent portion of vibrational energy of the reactants and products at 298.15 K, respectively. The calculated gas-phase enthalpy of proton is 5/2 (RT)=1.481 kcal mol^{-1} at 298.15 K. It corresponds to the translational proton energy (a loss of three degrees of freedom is 3/2(RT) plus the PV work-term (=RT for ideal gas).

Thermodynamically, GB is related to PA and the change of entropy ΔS at constant temperature (298.15 K) by Eq. 3:

$$GB = PA + T\Delta S. \quad (3)$$

For proton, only the translational entropy $S_{trans}(H^+)$ is not equal to zero and is determined to be 26.04 cal mol^{-1}K^{-1} [32].

In a solvent S, the reaction to be considered is identical to the one used in gas phase (1) except all constituents are solvated.

PA value is determined from PCM thermodynamic results, obtained from harmonic frequencies analysis, using Eq. 4.

$$PA = -\Delta_{prot}H = -\left[H\left(BH^+_{solv}\right) - H(B_{solv}) - H\left(H^+_{solv}\right)\right] \quad (4)$$

Compared to calculations in the gas phase, the only difference is for evaluation of proton enthalpy $H(H^+)$. The latter, independent of the base, is determined from summing the solvation enthalpy of the proton $\Delta_{solv}H(H^+)$ with proton gas-phase enthalpy $H\left(H^+_g\right)$ (1.48 kcal mol^{-1}). In aqueous solution, $\Delta_{aq}H(H^+)$ value (−275.14 kcal mol^{-1}) was determined experimentally by Tissander et al. using the cluster-pair based approximations [52]. Mejías and Lago determined this term theoretically and obtained a value of −275.12 kcal mol^{-1} [53], very close to Tissander experimental one.

Concerning the basicity in solution, the constant $pK_b(B)$ for a base B is given by the well known thermodynamic relation (5):

$$pK_b(B) = \frac{\Delta_{prot}G(sol)}{2.303\ RT}, \quad (5)$$

where R, T and $\Delta_{prot}G(sol)$ (1 atm, standard state) are the gas phase constant, the temperature (298.15 K) and the standard free enthalpy of base-protonation reaction in solution, respectively. $\Delta_{prot}G(sol)$ is determined from the following thermodynamic cycle

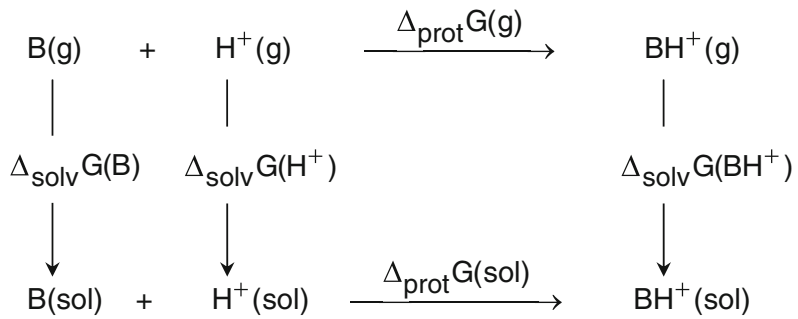

and is calculated by adding a solvation contribution $\Delta_{solv}G$ of each constituent to the gas phase basicity (Eq. 6):

$$\Delta_{prot}G(sol =)\Delta_{prot}G(g) + \Delta_{solv}G(BH^+) - \Delta_{solv}G(B) - \Delta_{solv}G(H^+) \quad (6)$$

In aqueous medium, the most reliable estimate of the experimental value for hydration of a proton $\Delta_{aq}G(H^+)$ is obtained from reference [52] and is equal to −264.23 kcal mol^{-1}. As developed in ref [54], this latter value concerns standard states essentially equal to 1 atm for gas and 1 M for solution. Thus, note that we must substract 1.9 kcal mol^{-1} to −264.23 kcal mol^{-1} to convert the cited standard conditions to 1 M/gas, 1 M/solution standard state [54]. Thus $\Delta_{aq}G(H^+)$ in water became −266.13 kcal mol^{-1}.

$\Delta_{prot}G(g)$ can also be calculated directly as follows:

$$\Delta_{prot}G(sol) = G(BH^+(sol)) - G(B(sol)) - G(H^+(sol)) \quad (7)$$

Note that in water, the aqueous free enthalpy $G(H^+(aq))$ is determined by summing $\Delta_{aq}G(H^+)$and $G(H^+(g))$, the latter being equal to −6.3 kcal mol^{-1} [55].

As to SO_2Cl_2 solvent, no experimental data is available. Thus, the evaluation of proton free enthalpy $G\left(H^+_{SO_2Cl_2}\right)$ and

proton enthalpy $H\left(H^{+}_{SO_2CI_2}\right)$ is performed from the difference between free enthalpies and enthalpies of SH^+ and S solvated species, respectively [32, 39]. Calculations lead to $G\left(H^{+}_{SO_2CI_2}\right) = -220.1 kcal\ \text{mol}^{-1}$ and $H\left(H^{+}_{SO_2CI_2}\right) = -219.3\ kcal\ mol^{-1}$.

Gas phase results and discussion

Molecular geometry and conformational preference

A complete geometry optimization has been carried out on the molecules both before and after carbonyl oxygen O* protonation.

High level theoretical calculations on the majority of unprotonated molecules in the gas phase have been performed [51]. *Verytight* and *Ultrafine* convergence criteria were adopted and no symmetry was imposed. For a few molecules, we were satisfied with standard convergence criteria. Whatever the substituent in para position may be, only one conformation is found stable. The corresponding conformer has a planar skeleton: the dihedral angle between the aromatic moiety and the acetyl group is zero or very close to zero, with two acetyl methyl protons staggered with respect to ortho proton.

Regarding the protonated forms, it was found that their ground state energies depend on the position of the hydroxyl group relatively to the methyl one. Four configurations (I, II, III, IV, Fig. 2) differing in positions of hydrogen atoms H_{15} and H_{18} are possible. The structure of each configuration was fully optimized in the gas phase. The absence of imaginary frequencies was checked in order to assess that the minimum conformation energy was reached. The stable minima forms are indicated for each compound in Table 1. The most stable conformation (minimum energy level value, in bold/Table 1) was used for the thermodynamical and structural calculations. The most prominent geometrical effects when going from neutral to protonated molecules will be discussed later together with the change of PA. It was found that, in general, protonated species with electron-withdrawing substituents tend to adopt form I (see Fig. 2) whereas form II is the conformational preference for derivatives with electron-donating substituents. Therefore, the phenyl ring and the oxygen lone pair are cis with respect to the carbonyl bond for both forms I and II. Note that the difference between energies of two stable forms for the considered derivatives is about 1.5−2.5 kcal.mol^{-1}: such energy difference cannot be ignored if accurate PAs are aimed, which justifies consideration and analysis of the four conformations.

Gas phase proton affinities and basicities

Before discussing the computational results, let us point out that some of the studied molecules should exhibit a second site of protonation, different from the carbonyl oxygen atom. All derivatives with X being or including a heteroatom with an electron lone pair (nitrogen, oxygen, sulfur) acting as an electron donor could be X-protonated. Proton affinities of these sites are inevitably different from those of the carbonyl oxygen. Table 2 shows that in all cases the carbonyl oxygen site has the highest affinity in gas phase. This conclusion corroborates low temperature NMR measurements in SO_2FCI solvent on p.X- acetophenones with X=OCH_3, CH_2OH [56].

Computed gas phase proton affinities PA and gas phase basicities GB for compounds under study are summarized in Table 1 together with experimental values. In this table, the molecules are arranged in decreasing order of their experimental PAs taken from NIST Standard Reference Database [48]. As indicated in the up to date tables of Hunter et al. [21], the uncertainty assigned to these experimental values is considered to be about 2 kcal mol^{-1}. Figure 3 depicts the plots of computed PAs versus the experimental ones. On inspection of these results, one observes that the computed thermodynamical values agree well with experiment with a mean absolute deviation equal to 3.5 kcal mol^{-1} and a mean relative deviation equal to 1.6 %. If one excludes PAs of N$(CH_3)_2$, NH_2 and SCH_3 compounds which are obviously overestimated by the method used, these deviations are lowered to 2.9 kcal mol^{-1} and 1.4 % respectively.

The proton affinity of unsubstituted acetophenone (X≡H) has been calculated by Taskinen et al. using various methods [33]. In their investigations, they showed that CCSD/6-311CG(d,p)//B3LYP/TZVP, G2(MP2) and G3(MP2)//B3LYP composite models gave PAs with the lowest absolute

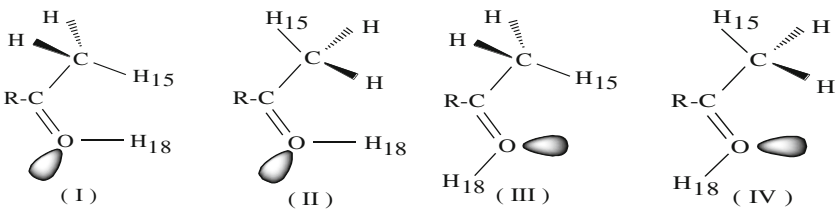

Fig. 2 Possible planar conformations for protonated acetyl fragment (R≡p.X−C_6H_4)

Table 1 Proton affinities (PA) and gas basicities (GB) of para-substituted acetophenones p.X−C_6H_4CO*CH_3 calculated (unscaled values) at B3LYP/6-311++G(2d,2p) level of theory, T=298.15 K

Substituent X	PA (kcal mol^{-1})		GB (kcal mol^{-1})		Stable forms *
	Calc.	Exp.	Calc.	Exp.	
$N(CH_3)_2$	228.3	222.8	220.8	216.6	(**II**)
NH_2	223.7	217.1	216.2	209.6	(**II**, III)
OCH_3	218.0	214.0	210.8	206.4	(**II**, III)
SCH_3	218.1	212.2	210.7	204.7	(**II**)
OH	215.1	211.1	207.8	203.6	(I, **II**, III)
$C(CH_3)_3$	214.6	210.8	207.7	203.3	(I, **II**, III)
CH_2OH	213.7	–	207.2	–	(**I**, III)
CH_3	213.1	209.2	206.4	201.6	(I, **II**, III)
H	208.9	205.7	202.3	198.2	(**I**)
Br	207.9	–	201.4	–	(I, **II**, III)
F	207.4	205.1	200.1	197.6	(**I**, III)
CI	207.6	204.6	201.4	197.1	(**II**, III)
I**	209.1	–	201.8	–	(**I**, III)
$COCH_3$	205.6	203.3	199.0	196.2	(**I**)
CF_3	201.5	199.9	193.5	192.4	(**I**)
CN	199.8	197.5	192.8	190.0	(**I**)
NO_2	197.4	196.9	190.5	189.4	(**I**)
$(CH_3)_2$ NH^+	141.6	–	134.1	–	(**I**)
CH_3SH^+	137.8	–	130.3	–	(**I**)
CH_3OH^+	137.2	–	129.9	–	(**I**)
$CH_2OH_2^+$	136.9	–	126.2	–	(**I**,III)
NH_3^+	136.5	–	128.9	–	(**I**)
OH_2^+	104.1	–	96.7	–	(**I**)

* most stable form in bold

** PA ang GB calculated at B3LYP/aug-cc-pVQZ-PP for iodine

deviation from experimental ones and concluded, as many other researchers [25, 31], that these models are computationally very expensive and therefore, not practical for molecules with more than about 12 heavy atoms. For larger systems, it may be necessary to sacrifice accuracy for computational efficiency. As sufficiently accurate methods which could be computationally much less demanding and applicable to larger molecules, they propose to use the combination method 1/2(DFT+MP2) consisting in evaluating the average of the proton affinities at the B3LYP/TZVP//B3LYP/TZVP and MP2/6-311+G(d,p)//B3LYP/TZVP levels. The resulting PA is very close to the experimental one.

When applying this combined approach to a series of several large molecules containing second and third-row atoms and considered in different conformations and in different states (gas phase, more or less polar solution-phase), calculations become rather expensive. In order to avoid such difficulties, using our computational procedures with an adequate scaling factor matching calculated with experimental data appears to be interesting. Application of a scaling factor equal to 0.983 balances the observed overestimation, leading to computed PAs values very close to experimental ones. As a matter of fact, a "chemical" accuracy of≈1 kcal mol^{-1} is often considered as satisfactory when treating large systems. Note

Table 2 Computed proton affinities PA (298.15 K, in kcal mol^{-1}) for different sites of protonation, other than carbonyl oxygen atom, in gas phase and in solution

ε (solvent)	Protonation site	**N**$(CH_3)_2$	**N**H_2	**O**H	CH_2**O**H
gas	O*	228.2	223.7	215.1	213.7
	X* [(a)]	218.4	204.3	173.5	194.2
(ε=9.15)	O*	_	42.8	37.0	34.6
	X*	_	36.9	10.3	_
(ε=78.8)	O*	− 7.6	− 7.2	− 12.2	− 15.0
	X*	− 6.1	− 11.0	_	− 23.4

[(a)] site of protonation in bold

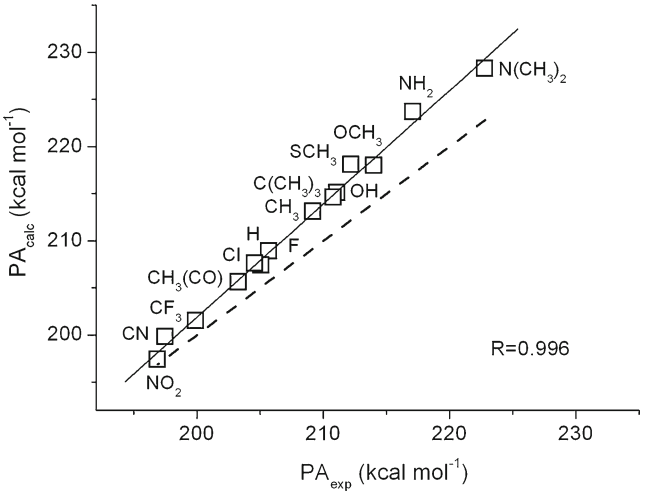

Fig. 3 Calculated proton affinities (in kcal mol^{-1}) versus experimental values in gas phase (298.15 K); (- - -): *diagonal line*, (——): *fitted line*

that scaling only the zero-point vibrational energy (ΔZPVE) rather the whole PA would be another alternative as was proposed in references [57, 58].

As has already been noticed, the adopted level of theory tends to weakly overestimate the thermochemical properties. Table 1 confirms this trend and shows that computed gas basicities agree with measured ones, with mean absolute and relative deviations of the same order of magnitude of those indicated for PAs. On the other hand, plot of $GB_{calc.}$ vs. $GB_{exp.}$ (Fig. 4) exhibits a quasi perfect linear correlation (R=0.993). Application of the same scaling factor (0.983) as proposed to match the calculated proton affinities with experimental ones leads to predicted GBs values very close to experimental ones.

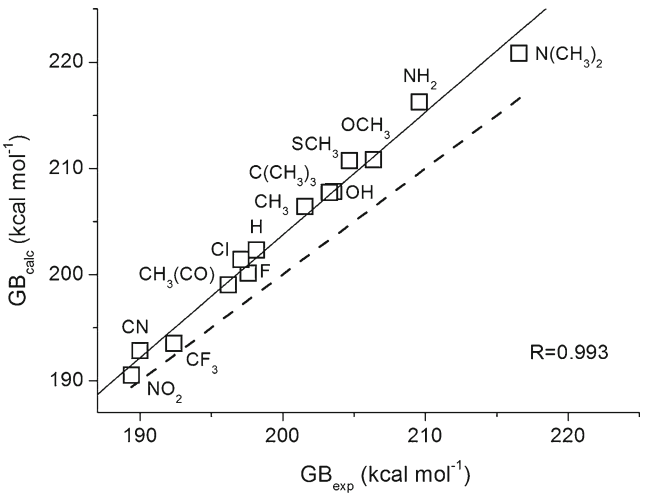

Fig. 4 Calculated GB basicities (in kcal mol^{-1}) versus experimental values in gas phase (298.15 K); (- - -): *diagonal line*, (——): *fitted line*

Substituent effects

Usually, substituent effects are analyzed with regard to Taft approach in which these effects are subdivided into three contributions [59]:

- the resonance (or mesomeric) effect measures the ability of the substituent to delocalize the π electrons to or from the rest of the molecule;
- the inductive and the field effects describe the electrostatic interactions between charges and multipoles (mainly the dipole) in the molecule; the first is transmitted by polarization of bonding electrons from one atom to the next one and the second is directly transmitted through space;
- the polarizability effect takes into account the electrostatic interaction between charges and induced multipoles (mainly the dipole) in the molecule.

Although separation of these contributions is quasi impossible, different strategies are adopted to achieve it [59]. When the considered system is aromatic and substituent X is a heteroatom, these strategies are very often applicable. Substituents considered in the series of compounds under study can be divided into different groups:

- $N(CH_3)_2$, NH_2 are highly electro-donating due to their heteroatom lone pair (SCH_3 and OCH_3 behavior is similar but less pronounced);
- F, Cl, Br, I are electron-withdrawing due to their polar effect one hand and electron-donating due to their resonance effect on the other hand, which leads to partial cancellation. The resulting effect on the electron circulation is modest and often comparable to the hydrogen one (taken as reference);
- CN, NO_2 are electron-withdrawing due to both inductive and mesomeric effects;
- cationic substituents $\overset{\oplus}{NH_3}$, . . . show charge and available electron lone pair deficit at the same time.

Being in para position, the considered substituents cannot exhibit any steric effect on the PAs and the other parameters. Their electronic characteristics only influence the electron organization in the molecular system. The substituent effects on the geometrical parameters of the unprotonated species have been investigated in an earlier paper [51]. The preferred conformation of the isolated molecule undergoes important changes on protonation. In the following, we would like to discuss possible correlation between X characteristics and computed properties: proton affinities, structural features and atomic charges.

i) Substituent effect on the molecular structure

The most noticeable geometrical changes during protonation would concern C_1-C_{12} and $C_{12}-O^*$ bonds.

Effectively, Table 3 in which are collected the corresponding bond lengths for both neutral and O*-protonated species together with O^*-H_{18} one, shows that these parameters display large variations when substituent X is changed. Note that results of only some substituents are reported in Table 3 in order to reduce the volume of the text; however, the whole series is taken into account in the related plots. From these data and those of Table 1, some identifiable trends could be pointed out. One can summarize them as follows:

- for a given substituent, protonation substantially shortens phenyl-acetyl bond length and increases carbonyl one. This fact can be explained with the aid of basic principles concerning electronic effects in the conjugated chemical systems. Here, whatever X may be, electron circulation is always toward the acetyl group, even if X is cationic. So, when the carbonyl oxygen atom is protonated, it acquires a more electron-accepting character than in the neutral form, which decreases the π character of the $C_{12}-O^*$ bond and increases the C_1-C_{12} one, leading to lengthening of the former and contraction of the latter. These variations seem somewhat more pronounced when X is a strong electron-donating substituent.
- in the protonated forms, the more the X substituent is electron-withdrawing, the longer the C_1-C_{12} bond length. As for the $C_{12}-O^*$ one, it varies in the opposite direction. As previously, these variations are due to conjugative interactions through the π-electron system between the aromatic moiety and the acetyl group. In the same way, the dominating influence of the mesomeric effect on electron migration toward the acetyl group allows to understand the weak shortening of the hydroxyl O^*-H_{18} bond when the electron-donating character of substituent X progressively increases.

ii) Correlation of substituent effect with atomic net charges

Effect of protonation manifests itself in the variation in electronic charge distribution in the protonated form relatively to neutral one. In the same way, for a given form, each substituent X affects the conjugative interactions and induces its own change in electron circulation. So, we can attempt to rationalize the effects of substituent X on the electron reorganization in terms of individual atomic properties as partial net charges. As there is no universally agreed upon best procedure for computing partial atomic charges, we prefer to discuss substituent effects according to two different schemes of population analysis: the Mulliken charge model whose population analysis is based on AO basis functions contributions to the overall wave function on the one hand and the Breneman-Wiberg charge model where atomic charges (called CHELPG charges) are computed based on analysis of the molecular electrostatic potential that is calculated from the wave function on the other hand [60].

As above, the most remarkable modifications concern O* and H_{18} atoms and, in lesser degree, the other atoms like C_{12}, . . . In Table 4, we have reported Mulliken and CHELPG net charges on these atoms for both gas phase unprotonated and O*-protonated forms and for only some representative substituents. Inspection of these results allows the following comments, whatever the considered charge scheme may be:

- local charge densities on all atoms, excepted H_{18} and in lesser degree O*, do not perfectly correlate

Table 3 Geometrical parameters of the neutral and O*-protonated forms in gas phase (length in Å) at the equilibrium ground state

Substituent X	d(C_1 C_{12})		d($C_{12}-O^*$)		d(O^*-H_{18})
	Neutral	Protonated	Neutral	Protonated	Protonated
$N(CH_3)_2$	1.483	1.391	1.220	1.327	0.966
NH_2	1.486	1.395	1.219	1.322	0.966
OCH_3	1.491	1.401	1.218	1.317	0.967
CH_3	1.496	1.412	1.217	1.310	0.968
H	1.499	1.420	1.216	1.302	0.969
CF_3	1.504	1.425	1.214	1.299	0.970
NO_2	1.506	1.429	1.213	1.297	0.970
$\overset{\oplus}{N}H(CH_3)_2$	1.518	1.449	1.209	1.286	0.974
$\overset{\oplus}{N}H_3$	1.521	1.455	1.209	1.284	0.974
$\overset{\oplus}{C}H_2OH_2$	1.529	1.452	1.208	1.285	0.974

Table 4 Computed CHELPG and Mulliken net charges (in a.u.) on C_{12}, O_{13} and H_{18} atoms for neutral and O*-protonated forms in gas phase, T= 298.15 K. $\Delta q_{O*H} = q(O_{13}) - 1 + q(H_{18})$ measures the electron migration toward the hydroxyl group

Charge	Nature	$N(CH_3)_2$	OCH_3	H	CF_3	NO_2	$(CH_3)_2NH^+$	NH_3^+
Neutral form								
$q(C_{12})$	Mulliken	0.495	0.511	0.478	0.464	0.505	0.477	0.488
	CHELPG	0.251	0.285	0.200	0.219	0.259	0.249	0.185
$q(O_{13})$	Mulliken	−0.527	−0.521	−0.499	−0.482	−0.488	−0.447	−0.444
	CHELPG	−0.481	−0.463	−0.451	−0.448	−0.431	−0.405	−0.397
O*-protonated form								
$q(C_{12})$	Mulliken	0.330	0.400	0.320	0.354	0.392	0.440	0.426
	CHELPG	0.670	−0.138	0.092	0.565	0.491	0.371	0.293
$q(O_{13})$	Mulliken	−0.466	−0.452	−0.392	−0.392	−0.394	−0.379	−0.366
	CHELPG	−0.302	−0.283	−0.277	−0.226	−0.220	−0.188	−0.193
$q(H_{18})$	Mulliken	0.444	0.445	0.448	0.453	0.454	0.473	0.473
	CHELPG	0.274	0.283	0.290	0.291	0.297	0.311	0.316
Charge variations (Δq)								
$\Delta q(O^*H)$	Mulliken	−1.022	−1.007	−0.944	−0.939	−0.940	−0.906	−0.893
	CHELPG	−1.028	−1.000	−0.987	−0.935	−0.923	−0.877	−0.877
$\Delta q(C_{12})$	Mulliken	−0.165	−0.111	−0.158	−0.110	−0.113	−0.037	−0.062
	CHELPG	0.419	−0.423	−0.108	0.346	0.232	0.122	0.108
$\Delta q(O_{13})$	Mulliken	0.061	0.069	0.107	0.090	0.094	0.068	0.078
	CHELPG	0.179	0.180	0.174	0.228	0.211	0.217	0.204

with the electronic characteristics (electron-donating/electron-withdrawing) of the substituents X. For H_{18} atom, although the change in net charge is small enough, an identifiable trend could be pointed out: the more the character of the substituent is electro-donating, the more important the migration of electrons toward carbonyl oxygen atom is and the weaker the positive charge on H_{18};

- change in electron density on the oxygen atom ($\Delta q(O^*)$) accompanying the protonation does not seem very affected by the nature of the substituent, in opposition to ($\Delta q(C_{12})$) which is widely affected and the resulting effect is not clearly related to electronic characteristics of the substituent X;
- by another way, electron migration toward the hydroxyl group in the protonated form, given by the sum $\Delta q_{O*H} = [q(O*) - 1 + q(H_{18})]$, is nearly not influenced by the nature of the substituent and is nearly twice the one toward oxygen atom in neutral form (≈−0.89, −1.02 a.u.against≈−0.44, −0.53 a.u.). So, CO* protonation substantially increases the electron deficit of the rest of the molecule.

iii) correlation of substituent effect with proton affinity

The proton affinities of molecules similar to those under study are determined by different factors. However, two are essential:

- the charge density on the proton acceptor site,
- the conjugative interactions in the molecule and the protonated species.

For the considered molecules, the electron delocalization without doubt plays the most important role by enhancing/diminishing the electron density in the system.

From the data in Table 1, one can observe that the gas phase proton affinity displays very large variations with substitution in para position. The trend is clear: the more the character of the substituent is electro-donating, the higher the proton affinity. $N(CH_3)_2$ being the strongest electron-donating, its effects are quantitatively transmitted to the protonation site, which explains the high value of the corresponding PA value. On the contrary, NO_2 and CN substituents lead to weaker values. The most remarkable fact in Table 1 is the drastic decrease of the proton affinity when the substituent X is positively charged (PA values corresponding to $\overset{\oplus}{OH_2}$ is lower than the half of $N(CH_3)_2$). Onecan explain this dramatic diminution by inspecting

change of electron densities on the proton acceptor sites in the Born-Haber cycle of cationic X substituent derivatives.

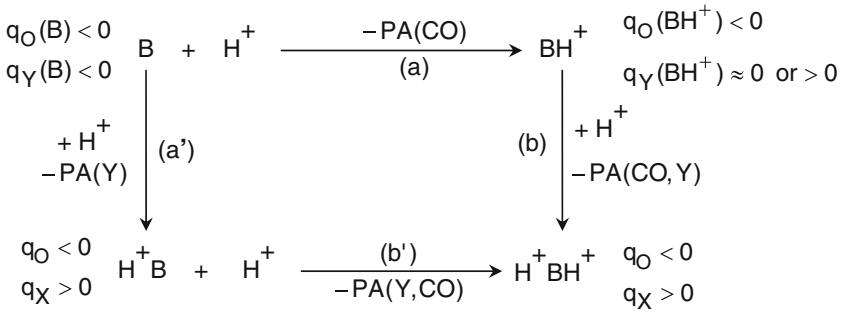

The different symbols have the following significance :

- B refers to neutral molecule p.Y−$C_6H_4CO^*CH_3$,
- Y is the X conjugate base :X≡YH^+
- BH^+ (H^+ on the right hand-side of B) is the O*-protonated form (cation),
- H^+B (H^+ on the left-hand-side of B) is the Y-protonated form (cation),
- H^+BH^+ is the dication form.

The protonation site is indicated in parentheses. When two sites are concerned, the first to be protonated is placed in the first position. Hess' law allows to write:

$$PA(Y, CO*) = PA(CO*) - PA(Y) + PA(CO*, Y) \qquad (8)$$

Table 2 shows that the proton affinities PA(CO*) and PA (Y) are both high (≈200 kcal mol^{-1}) due to the important negative charges on both carbonyl oxygen and X atoms (more precisely on heteroatom bonded to the phenyl ring) and the corresponding steps (a) and (a') are not highly energetic, contrary to step (b) for which a high energetic price has to be paid. As a matter of fact, step (a) substantially weakens the charge $q_Y(BH^+)$ on the heteroatom. For instance, this remaining charge is positive for Y≡$N(CH_3)_2$ and≈−0.15 a.u. for Y≡NH_2. Consequently, step (b) proton affinity PA (CO*, Y) is expected to be low compared to those cited above, and this is confirmed by computations: for example, the calculated PA (CO*, NH_2) is only 117.1 kcal mol^{-1}.

All the preceding results indicate that electronic characteristics of the substituent correlate with the change in most properties of the system. We can now attempt to rationalize the substituent effects by plotting computed PA versus structural parameters and atomic charges. Figure 5 shows that whatever the substituent X, PA is in very good linear relationship with oxygen-hydrogen bond length in the protonated form whereas a similar correlation with carbon-oxygen bond length can be observed only if cationic substituents are excluded. In the same way, Fig. 6 shows that plots of PA versus Mulliken and CHELPG net charges on oxygen atom before and after protonation from one hand and those on hydrogen H_{18} on the other hand could display some correlation. If only Mulliken charges in neutral substituents X derivatives are taken into account, correlation tends to be linear (R=0.97 and 0.92 before and after protonation, respectively) (Fig. 6).

All things considered, it seems that explanation of cationic substituent effects with the aid of only conjugative interactions and charge density on the proton acceptor site is insufficient.

Solvent effects

The above calculated properties refer to the gas phase. Para-substituted acetophenones have not been abundantly investigated in various solvents. Among the few papers concerning

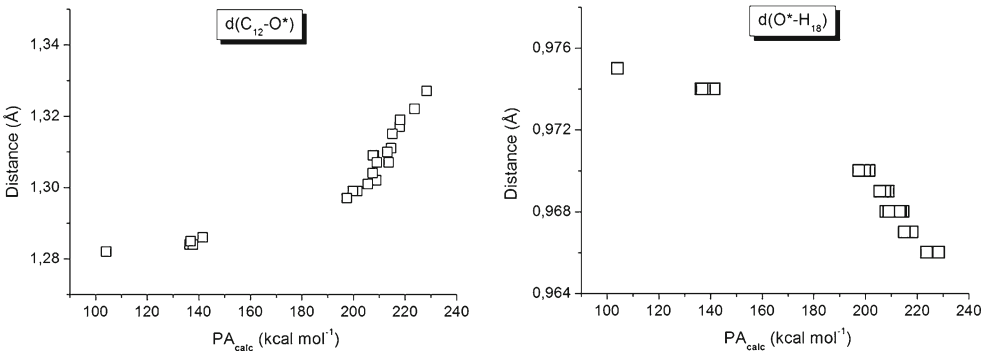

Fig. 5 Calculated proton affinities (in kcal mol^{-1}) versus C_{12}−O* and O*−H_{18} bond lengths (in Å) in gas phase protonated forms

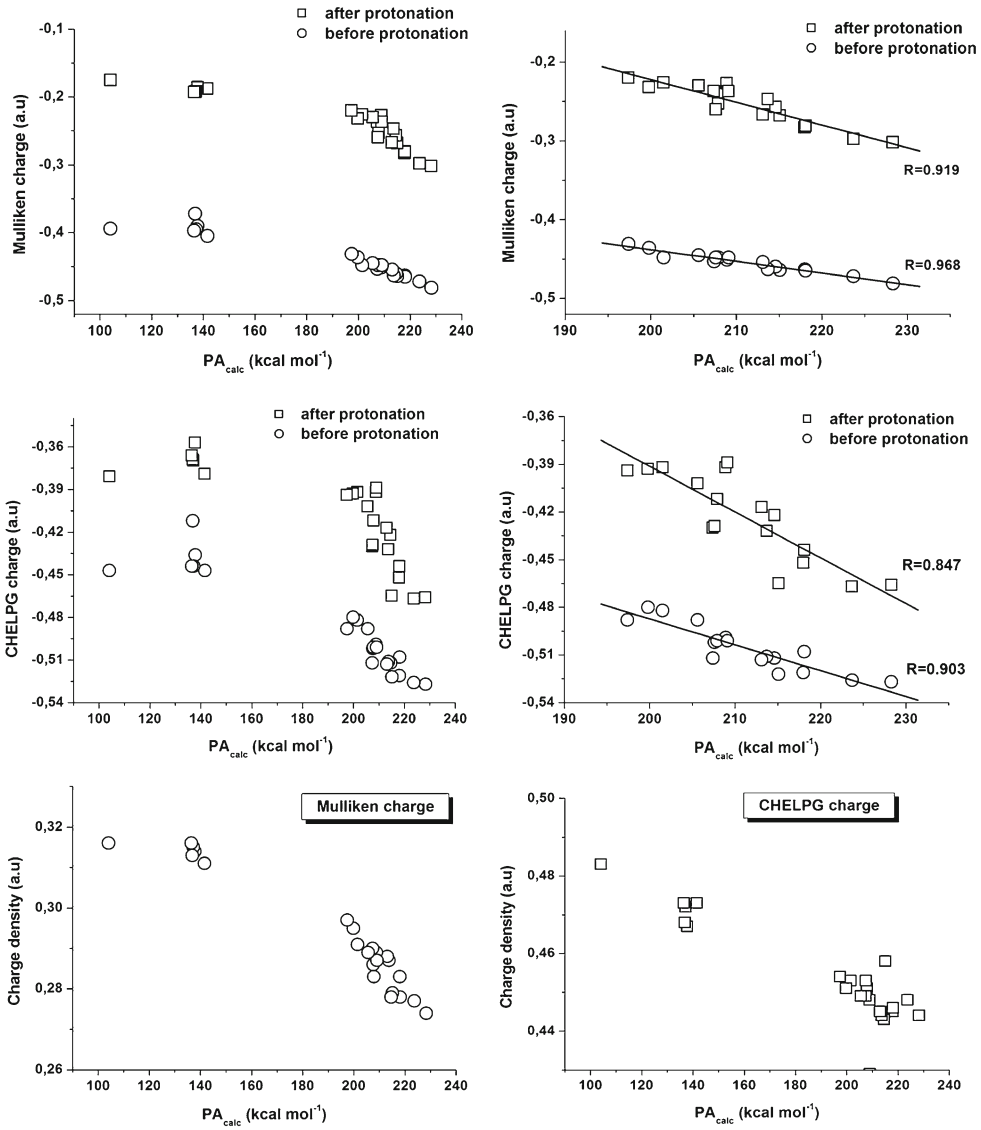

Fig. 6 Calculated PAs (in kcal mol^{-1}) vs. atomic net charge (in a.u.) in gas phase (*Top*) vs. Mulliken charge on carbonyl oxygen atom before and after O*-protonation (*Middle*) vs. CHELPG charge on carbonyl oxygen atom before and after O*-protonation (*on the left*): all substituents X; (*on the right*): only neutral substituents (*Bottom*) vs. charge density on hydrogen hydroxyl atom H_{18}

protonation of these compounds, the following include the most important results:

- the first protonation pK(B) measurements concern the protonation equilibria of unsubstituted acetophenone and are in the range *3.9→8* [10–13];
- more recently, pK(B) of p.X-substituted acetophenones with X≡H, F, Br, CH_3, OCH_3, CF_3, CN, NO_2 in aqueous sulfuric acid at 298 K were measured [14]. The corresponding pK(B) values are reported in Table 5.

To discuss theoretically the influence of the environment on PAs, pK(B) and others properties of p.substituted acetophenones, calculations have been carried out for two media: in aqueous solution (water is high dielectric solvent with ε= 78.8 and for which thermodynamic parameters are available as indicated above) and in SO_2CI_2 solution. The latter has been chosen because it is a low permittivity medium on the one hand and on the other hand because a low temperature (253 K) carbon-13 NMR study, aiming to determine the barrier of internal rotation around the phenyl-acetyl group [56], has shown that superacids could protonate weak bases like carbonyl compounds under study to form stable salts in non aqueous solution. Actually, in the corresponding experimental study, SO_2ClF (and not SO_2CI_2) was used as solvent and the protonating agent was the 1:1 magic acid (equimolecular mixture of fluorosulfonic acid FSO_3H and antimony pentafluoride SbF_5). Nevertheless, as the dielectric constant of liquid SO_2ClF has not been reported in literature and is presumably low and probably of the same order as the SO_2CI_2 one (ε=9.15), so, in the following, the computations relative to weak dielectric solvent effects refer to temperature 253 K and ε=9.15.

There are several possibilities of how to theoretically investigate solvation effects. As the self consistent reaction

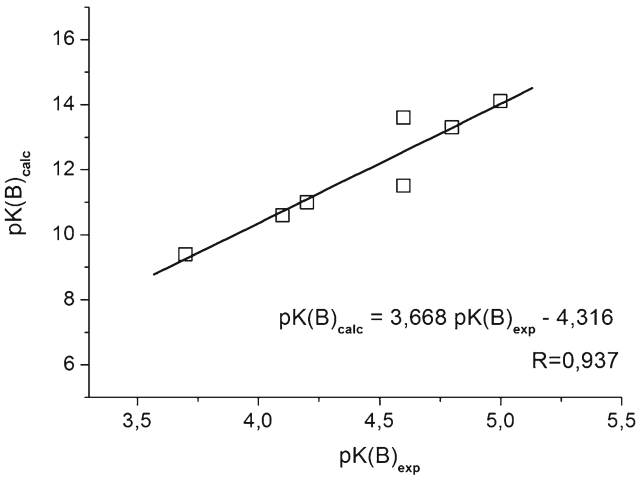

Fig. 7 $pK(B)_{calc}$ vs. $pK(B)_{exp}$ for experimentally studied acetophenones (ref [14]) in high ε medium ε=78.80

field (SCRF) continuum solvation method using IEF-PCM model has been reported to be more reliable in calculating proton affinities [40] on the one hand, and is the less problematic in parametrization and convergence on the other hand, we have chosen to discuss solvent effects on protonation with respect to the cited approach at DFT/6-311++G(2d,2p) level of theory. It was effectively demonstrated that this method, which is not expensive, leads to reliable barriers of internal rotation in both unprotonated and protonated p.substituted acetophenones [51, 61]. All the gas phase structures were reoptimized. In general, performing calculations with default cavity parameters (UA0 radii model, electrostatic scaling factor equal to 1.2) linked to Gaussian03, we have encountered no serious convergence problem, except in some cases. By successive modifications of the initial geometrical parameters, we have been able to characterize the stationary points whatever the solvent. Let us comment briefly on the most important aspects of the computed solvent effects.

Preferred protonation site

As shown previously, the presence of heteroatom (X) suggests a second site of protonation besides carbonyl oxygen atom (CO*). Relative probabilities of CO* and X protonation reactions are not a priori the same as in the gas phase. Computed PAs of the most probable sites are listed in Table 2 for the two considered mediums. These values indicate that carbonyl oxygen still remains the most basic site in solution as in gas phase except for $N(CH_3)_2$ substituent in high dielectric medium where nitrogen seems to be a little easier to protonate. However this result cannot be verified because of lack of experimental data, for the other substituents in SO_2ClF and in presence of superacid it was shown that the oxygen atom is the easiest to

Table 5 Proton affinities (PA, kcal mol^{-1}) and basicities (pK(B)) of para-substituted acetophenones p.X−$C_6H_4CO^*CH_3$ calculated at B3LYP/6-311++G (2d,2p) level of theory. (solvents: H_2O, SO_2ClF; temperature: 298 K)

Substituant	H_2O(aqueous solution)			SO_2ClF			Exp(pK(B))	
	PA	$\Delta_{prot}G$	pK(B)	PA	$\Delta_{prot}G$	pK(B)	*	**
NH_2	− 7.2	5.5	4.0	42.8	− 42.4	− 36.4		
$N(CH_3)_2$	− 7.6	6.1	4.5	_	_	_		− 1.8
OH	− 12.2	10.6	7.7	37.0	− 36.6	− 31.4		
SCH_3	− 13.3	11.2	8.2	_	_	_		
CH_3	− 14.8	12.9	9.4	_	_	_	3.7	
CH_2OH	−15.0	13.3	9.7	34.6	− 34.1	− 29.3		
H	− 16.2	14.5	10.6	32.8	− 32.2	− 27.6	4.1[(a)]	− 1.1
F	− 16.5	15.1	11.0	32.2	− 31.6	− 27.1	4.2	
CI	− 17.0	15.6	11.4	31.7	− 31.1	− 26.7		− 0.9
Br	− 17.2	15.8	11.5	31.5	− 31.0	− 26.6	4.6	
I[(b)]	− 18.7	16.8	12.2	30.0	− 29.9	− 25.6		
CF_3	− 19.4	18.2	13.3	28.7	− 28.8	− 24.7	4.8	
CN	− 20.0	18.7	13.6	27.9	− 27.2	− 23.3	4.6	
NO_2	− 21.1	19.8	14.4	26.6	− 25.9	− 22.2	5.0	
$\overset{\oplus}{C}H_2OH_2$	− 19.9	18.2	13.3	_	_	_	_	
$\overset{\oplus}{N}H_3$	− 20.6	18.8	13.7	22.4	− 22.1	− 18.9		
$\overset{\oplus}{N}H(CH_3)_2$	− 21.0	19.6	14.3	_	_	_	_	
$\overset{\oplus}{S}HCH_3$	_	_	_	20.9	− 21.6	− 18.5		
$\overset{\oplus}{O}H_2$	_	_	_	21.9	− 20.6	− 17.7		

* in aqueous sulfuric medium [14]; ** in CCI_4 medium [1]

[(a)] other measured pK(B) values: pK(B)=3.9 ref [10]; pK(B)=6.0 ref [11]; 6.5 ref [12]; pK(B)=8.0 ref [13]

[(b)] calculated at B3LYP/aug-cc-pVQZ-PP for iodine

protonate [56]. In high dielectric solvent, the highly negative PA value corresponding to CH_2OH substituent predicts that this derivative would not be capable of protonation on its hydroxyl oxygen atom. All these calculations allow us to conclude that in low dielectric solvent, X-protonation is possible but less favorable than O*-one whereas in high dielectric medium, it is more energy demanding than O*-protonation and very dependent on the nature of X.

Note that NO_2 group can be a proton acceptor in strong superacids. By measuring the different NMR chemical shifts of paranitroacetophenone dissolved in pure $FSO3_H$ acid and correlating them with Brown's σ^+ constants, it was demonstrated that in this medium, this compound is monoprotonated on the carbonyl oxygen atom [56].

Solvent effects on proton affinity

Proton affinities and basicities of compounds under study, calculated according to procedure section, are gathered in Table 5. The large basicity range exhibited in this table is evidently the result of cooperation of both induced solvent effects (solvation) and substituent effects. However, inspection of these results reveals that solvation is enormous in influencing these thermodynamic properties in solution whereas substituent effect is much less large.

The most remarkable result is certainly the drastic change of PA and GB when going from the gas phase to solvent. Whatever the substituent, protonation of the considered compounds in solution is much more difficult than in gas phase. The reason of this drastic diminution must be searched for in expression (4) used to calculate the proton affinity in solution. As a matter of fact, in this equation the enthalpy difference $H\left(BH^+_{solv}\right) - H(B_{solv})$ is of the same order of magnitude as its homolog in gas phase: the former is in the range [−266→−253] kcal.mol^{-1} and the latter in the range [−227→−196] kcal mol^{-1}; so proton affinities are about 200 kcal mol^{-1}. On the contrary, the proton enthalpy in solution $H\left(H^+_{solv}\right)$ is equal to −219.3 kcal mol^{-1} for SO_2CI_2 and −273.66 kcal mol^{-1} for H_2O (see Computational procedures section) whereas its homolog in gas phase (5/2 (RT)) is only≈1.5 kcal mol^{-1}. This difference in proton enthalpies on going from gas to solution explain the dramatic decrease of PA accompanying solvation.

Table 5 shows that proton affinity increases and pK(B) decreases when the permittivity of the medium is reduced, which means that studied carbonyl compounds are more difficult to protonate in aqueous solution than in organic solvents. This conclusion is in qualitative agreement with other experimental observations: in their work on substituted phenols, Klein et al. have calculated PAs in both water and benzene [39] and found the same PA arrangement: $PA_g >> PA_{C_6H_6} > PA_{H_20}$.

The effect of substituent on proton affinity shows the same trend as in gas phase. In both solvents, electro-releasing substituent effect algebraically raises PAs and lowers pK(B)s. In water, the considered series of carbonyl compounds experiences a basicity increase of about 10 pK (B) units on going from the nitro to the amino derivative and of 14 units in SO_2CI_2 medium. Although these values are probably excessive, they show that the magnitudes of substituent effects are not comparable and exhibits some correlation with electro-donor/electro-acceptor properties of X substituents. For a given substituent whose electronic properties are known, it should even be possible to predict the probable pK(B) value of corresponding derivative.

Confrontation of computed pK(B) values with experiment allows us to form the following comments.

– On inspection of Table 5, one can realize that quantitative agreement between theory and experiment is poor for both solvents. Let us take an interest in the more recent pK(B) measurements due to Chimichi et al. [14]. These values, determined in same conditions (298 K, in aqueous sulfuric acid solution by U.V. spectroscopy) are to be compared with computed $pK(B)_{calc,aq}$. Plot of $pK(B)_{calc,aq}$ vs. $pK(B)_{exp}$ (Fig. 7) exhibits qualitative agreement. If one assumes linear behavior, the fitted equation should be given by the following expression:

$$pK(B)_{calc} = 3.668 pK(B)_{\exp} - 4.316 (R = 0.937) \qquad (9)$$

This value of the correlation coefficient R is not representative of a true linear relation (for which R≥0.99). Nevertheless, it is indicative of a quasi linear correlation.

– Among all carbonyl compounds unter study, unsubstituted acetophenone is the most investigated derivative [10–14]. Noting the large differences between $pK(B)_{exp,aq}$ values known in the literature (*3.9→8.0*), our calculated value (10.6) is close to the highest extremity (8.0) [13].
– In the literature, there is no available value of pK(B) corresponding to SO_2CI_2 medium. On the other hand, there are some pK(B) data measured in CCI_4 solution [1]. These two solvents are not chemically similar (polarities are different, . . .); nevertheless, their permittivities are of the same order. So, confrontation of calculated $pK(B)_{calc,}SO_2CI_2$ can take place with $pK(B)_{exp,}CCI_4$. Results listed in Table 5 exhibit excessively large discrepancies between theory and experiment. These differences are very much larger than those observed for aqueous solution. In our opinion, these anomalies are due to the fact that theoretical proton free enthalpy $G\left(H^+_{SO_2Cl_2}\right)$ is badly evaluated (−220.1 kcal mol^{-1}) by the difference of free enthalpies $G(SO_2Cl_2H^+)_{SO_2Cl_2} - G(SO_2CI_2)_{SO_2Cl_2}$.

Furthermore, if $G\left(H_{aq}^{+}\right)$ has been calculated in a similar manner, one would find a value of nearly (−244 kcal mol^{-1} whereas the best value is (−272.43 kcal mol^{-1} (Computational procedures section): such a difference, equal to≈28 kcal mol^{-1}, is indeed very large. So, it appears that used computational method underestimates the absolute value of proton free enthalpy in SO_2CI_2. If a similar quantity (≈28 kcal mol^{-1}) is added to $\Delta_{prot}G_{SO_2Cl_2}$ values of Table 5, calculated pK(B) values for acetophenone and p.chloro-acetophenone become equal to −3.7 and −2.7, respevtively (against experimental values in CCI_4: −1.1 and −0.9 [1]). Finally, one can conclude that the computation of the proton free enthalpy in solution with high accuracy is fundamental in solvation study if reliable experimental data are not available.

Computed properties vs. solvent effects

It is worthwhile to discuss some details concerning changes in other computed parameters when going from unprotonated to protonated compounds in solution. Once more, the whole results were not listed in the tables; however, they were taken into account in the related plots.

Structural properties

The structural features at or around the carbonyl group in solution are considered to be compared to those in gas phase. Values of C_1-C_{12}, $C_{12}-O^*$ and O^*-H_{18} bond lengths display variations with substituent electronic properties comparable to those in the isolated state for both unprotonated and protonated forms. Thus interpretation, previously given to explain the gas phase results, still works. Nevertheless, a point could be at least mentioned: for the same substituent, increasing the dielectric constant of the medium shortens $C_{12}-O^*$ and lengthens C_1-C_{12} and O^*-H_{18}.

Partial net charges

The Mulliken and CHELPG net charges q(O*) on the carbonyl oxygen atom both before and after protonation as well as on acidic hydrogen $q(H_{18})$ are partially summarized in Table 6. Some trends are worth pointing out.

– Whatever the environment, oxygen atom still remains negatively charged for all compounds after protonation

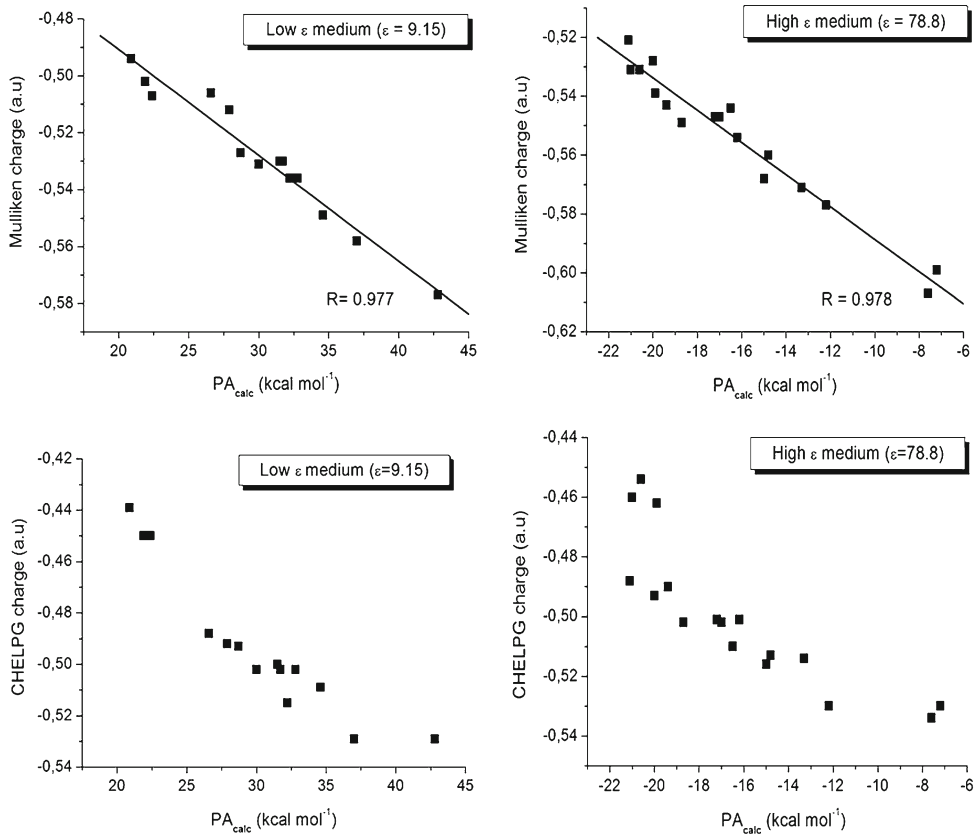

Fig. 8 Calculated PAs (kcal mol^{-1}) vs. net charge on carbonyl oxygen atom in solution (for two dielectric constants :ε=9.15, ε=78.80) before O*-protonation. (*Top*) vs. Mulliken net charge. (*Bottom*) vs. CHELPG net charge

Table 6 Computed CHELPG and Mulliken (in parentheses) net charges (in a.u.) on C_{12}, O_{13} and H_{18} atoms for neutral and O*-protonated forms in solution, T=298.15 K

Charge	Nature	NH_2	CH_2OH	H	CF_3	NO_2	NH_3^+	OH_2^+
High dielectric medium (ε=78,8)								
Neutral form								
$q(C_{12})$	Mulliken	0.283	0.296	0.268	0.275	0.319	0.241	_[a]
	CHELPG	0.491	0.496	0.473	0.484	0.490	0.497	_
$q(O_{13})$	Mulliken	− 0.599	− 0.569	− 0.554	− 0.543	− 0.521	− 0.531	_
	CHELPG	− 0.530	− 0.516	− 0.501	− 0.490	− 0.488	− 0.454	_
O*-protonated form								
$q(C_{12})$	Mulliken	0.544	0.627	0.145	0.420	0.533	0.344	0.272
	CHELPG	0.400	0.390	0.376	0.411	0.425	0.452	0.422
$q(O_{13})$	Mulliken	− 0.346	− 0.272	− 0.253	− 0.242	− 0.233	− 0.243	− 0.231
	CHELPG	− 0.473	− 0.408	− 0.398	− 0.397	− 0.396	− 0.374	− 0.363
$q(H_{18})$	Mulliken	0.336	0.358	0.362	0.370	0.373	0.371	0.370
	CHELPG	0.450	0.447	0.454	0.459	0.461	0.477	0.477
Low dielectric medium (ε=9.15)								
Neutral form								
$q(C_{12})$	Mulliken	0.268	0.295	0.256	0.265	0.309	0.229	0.240
	CHELPG	0.493	0.496	0.476	0.493	0.496	0.494	0.494
$q(O_{13})$	Mulliken	− 0.577	− 0.549	− 0.536	− 0.527	− 0.506	− 0.507	− 0.503
	CHELPG	− 0.529	− 0.509	− 0.502	− 0.493	− 0.488	− 0.450	− 0.450
O*-protonated form								
$q(C_{12})$	Mulliken	0.543	0.617	0.137	0.604	0.527	0.337	0.271
	CHELPG	0.380	0.388	0.340	0.403	0.420	0.449	0.431
$q(O_{13})$	Mulliken	− 0.337	− 0.266	− 0.247	− 0.239	− 0.229	− 0.232	− 0.220
	CHELPG	− 0.469	− 0.409	− 0.391	− 0.396	− 0.396	− 0.373	− 0.367
$q(H_{18})$	Mulliken	0.324	0.343	0.347	0.352	0.358	0.359	0.358
	CHELPG	0.451	0.446	0.452	0.458	0.460	0.476	0.477

[a] Convergence has not been obtained

reaction. Net charge results show a decrease for q(O*) values before as well as after protonation when going from electron-donor to electron-withdrawing substituents. The reverse is observed for $q(H_{18})$.

– For a given substituent, the CHELPG pre- and post-protonation electron densities q(O*) are nearly independent of the dielectric constant whereas Mulliken ones weakly increase with ε. For proton H_{18}, its CHELPG charge remains constant and its Mulliken one is more positive when ε increases.

As in gas phase, we conclude this solvent effect study by plotting computed PAs versus net charges q (O*) in the different mediums, before protonation. Figure 8 exhibits clear linear correlation between PAs and Mulliken q(O*) charges in the unprotonated forms, even if values associated with the cationic substituents are not excluded. Correlation coefficients are nearly equal to 0.98. On the contrary, the behavior of CHELPG oxygen net charges does not exhibit a clear linear relation to proton affinities.

Possible amelioration of the computational method

The computational method adopted in these investigations nearly works well in evaluating gas phase proton affinities and basicities. So, one should think that the disagreement between theory and experiment in calculating pK(B) is not due to the method itself, but rather to parametrization of the molecular cavity and, why not, to the choice of the PCM model (IEF-PCM, C-PCM, D-PCM, . . .). Results of Table 5 were obtained using the united atom topological model UA0 where the atomic radii arise from FFF force field. Barone et al. have shown that this model does not allow to reproduce experimental results even if Bondi or Pauling radii are used [62]. They proposed to define the cavity according to UAHF

(as implemented in Gaussian03 code). Other authors used the C-PCM and D-PCM solvation models with UAHF or UAKS cavities [63–65]. All these methods led to better results than the standard PCM model.

Concerning the present solvent effect study on proton affinity and basicity of p.substituted acetophenones, we have tested the above cited formalisms only on unsubstituted acetophenone. With the Gaussian03 code, we have encountered serious difficulties in convergence.

Finally, the DFT(B3LYP)/6-311++G(2d,2p) method used in these investigations is distinguishable from others by the fact that it is not at all onerous and, consequently, can be used to study series of too large molecular systems in a systematic manner for a comparison of their properties. Without no doubt, the true improvement in calculating accurate proton affinities and basicities consists in use of more elaborated computational methods (CCSD(T), . . .) or other solvation formalisms (SMD, . . .) [66]. Unfortunately, such levels of theory are expensive.

Conclusions

The present investigations on proton affinity and structural properties of a series of para-substituted acetophenones in the gas phase and in solution allowed to draw the following conclusions:

- accurate PA values could be achieved using computational methods which are much less demanding than more sophisticated ones. DFT(B3LYP) method with 6-311++G(2d,2p) basis was shown to yield satisfactory results on condition of some scaling factors and could be successfully applied to a wide series of large containing carbonyl molecules;
- in all studied molecules, whatever the substituent in para position, the carbonyl oxygen atom is the preferential protonation site. A second protonation on X substituent heteroatom is also possible;
- proton affinities are directly influenced by the electron-donating/withdrawing character of the substituent. Protonation induces migration of electrons from all over the molecular system leading to pronounced charge redistributions compared to pre-protonation one;
- in gas phase, generally proton affinity is nearly in linear relationship with structural and electronic charge properties of the carbonyl group before and after protonation.
- in solution, the most remarkable result is certainly the drastic change of proton affinity on going from gas to solution phase. This indicates that protonation is not energetically favorable in liquid phase.
- computed pK(B)values in aqueous solution are in good qualitative agreement with experiment. Nevertheless, they exhibit discrepancies with regard to measured ones.
- in organic solvent, knowledge of the proton free enthalpy with high accuracy is fundamental in solvation study if reliable experimental data are not available.

References

1. Carrasco N, González-Nilo F, Caroli Rezende M (2002) Tetrahedron 58:5141–5145
2. Wolken JK, Tureček F (2000) J Am Soc Mass Spectrom 11:1065–1071
3. Jursic BS (1999) J Mol Struct (THEOCHEM) 490:1–6
4. Sun W, Kinsel GR, Marynick DS (1999) J Phys Chem A 103:4113–4117
5. Strittmatter EF, Williams ER (1999) Int J Mass Spectrom 185–187:935–948
6. Eckert-Maksić M, Klessinger M, Maksić ZB (1995) Chem Phys Lett 232:472–478
7. Rivera A, Moyano D, Maldonado M, Ríos-Motta J, Reyes A (2009) Spectrochim Acta Part A 74:588–590
8. Chandra AK, Goursot A, Fajula F (1997) J Mol Catal A Chem 119:45–50
9. Yates K, Stewart R (1959) Can J Chem 37:664–671
10. Bagno A, Lucchini V, Scorrano G (1991) J Phys Chem 95:345–352
11. Culbertson G, Pettit R (1963) J Am Chem Soc 85:741–743
12. Haake P, Cook RD, Hurst GH (1967) J Am Chem Soc 89:2650–2654
13. Greig CC, Johnson CD (1968) J Am Chem Soc 90:6453–6457
14. Chimichi S, Dell'Erba C, Gruttadauria M, Noto R, Novi M, Petrillo G, Sancassan F, Spinelli D (1995) J Chem Soc Perkin Trans 2:1021–1026
15. Ebrahimi A, Habibi-Khorasani SM, Jahantab M (2011) Comput Theor Chem 966:31–37
16. Oteypková E, Nevěčná T, Kulhánek J, Exner O (2003) J Phys Org Chem 16:721–725
17. Kukol A, Strehle F, Thielking G, Grötzmacher H-F (1993) Org Mass Spectrom 28:1107–1110
18. Choi KH, Lee HJ, Karpfen A, Yoon CJ, Park J, Choi YS (2001) Chem Phys Lett 345:338–344
19. Hodges RV, Beauchamp JL, Ashe AJ, Chan WT (1985) Organometallics 4:457–461
20. Böhm S, Gal JF, Maria PC, Kulhánek J, Exner O (2005) Eur J Org Chem 2580-2588
21. Hunter EPL, Lias SG (1998) J Phys Chem Ref Data 27:413–656
22. Meot-Ner (Mautner) M (2003) Int J Mass Spectrom 227:525–554
23. van Beelen ESE, Koblenz TA, Ingemann S, Hammerum S (2004) J Phys Chem A 108:2787–2793
24. Noguera M, Rodríguez-Santiago L, Sodupe M, Bertran J (2001) J Mol Struct (THEOCHEM) 537:307–318
25. Deakyne CA (2003) Int J Mass Spectrom 227:601–616
26. Kalbi S, van Beelen ESE, Ingemann S, Henriksen L, Hammerum S (2006) Int J Mass Spectrom 249–250:370–378
27. Kovaček D, Maksić ZB, Novak I (1997) J Phys Chem A 101:1147–1154
28. Maksić ZB, Kovačević B, Kovaček D (1997) J Phys Chem A 101:7446–7453
29. Wróblewski T, Ziemczonek L, Szerement K, Karwasz GP (2006) Czech J Phys 56:B1110–B1115
30. Bruno G, Nicolò F, Tresoldi G, Lanza S, Rotondo A (2007) J Mol Struct (THEOCHEM) 818:131–139

31. Jursic BS (1999) J Mol Struct (THEOCHEM) 487:193–203
32. Raczyńska ED, Makowski M, Górnicka E, Darowska M (2005) Int J Mol Sci 6:143–156
33. Taskinen A, Nieminen V, Toukoniitty E, Mursin DY, Hotokka M (2005) Tetrahedron 61:8109–8119
34. Hadjadj-Aoul R, Bouyakoub A, Krallafa A, Volatron F (2008) J Mol Struct (THEOCHEM) 849:8–16
35. Namazian M, Coote ML (2008) J Chem Thermodyn 40:1627–1631
36. Namazian M, Coote ML (2008) J Chem Thermodyn 40:1116–1119
37. Pokon EK, Liptak MD, Feldgus S, Shields GC (2001) J Phys Chem A 105:10483–10487
38. Tajkhorshid E, Paizs B, Suhai S (1997) J Phys Chem B 101:8021–8028
39. Klein E, Rimarčík J, Lukeš V (2009) Acta Chimi Slovaca 2:37–51
40. Hilal R, Abdel Khalek AA, Elroby SAK (2005) Int J Quantum Chem 103:332–343
41. Senapati U, De D, De BR (2008) Indian J Chem 47A:548–550
42. Senapati U, De D, De BR (2007) J Mol Struct (THEOCHEM) 808:153–155
43. Swart M, Bickelhaupt FM (2006) J Chem Theor Comput 2:281–287
44. Pandit S, De D, De BR (2006) J Mol Struct (THEOCHEM) 778:1–3
45. Rinaldi D, Rivail JL (1973) Theor Chim Acta 32:57–70
46. Rivail JL, Rinaldi D (1976) Chem Phys 18:233–242
47. Miertus S, Scrocco E, Tomasi J (1981) Chem Phys 55:117–129
48. NIST: National Institute of standards and Technology Reference Database available at www.webbook.nist.gov
49. Frisch MJ et al. (2003) Gaussian 03, Revision B 04. Gaussian, Pittsburgh
50. Peterson KA, Shepler BC, Figgen D, Stoll H (2006) J Phys Chem A 110:13877–13883
51. Haloui A, Arfaoui Y (2010) J Mol Struct (THEOCHEM) 950:13–19
52. Tissandier MD, Cowen KA, Feng WY, Gundlach E, Cohen MH, Earhart AD, Coe JV, Tuttle TR Jr (1998) J Phys Chem A 102:7787–7794
53. Mejías JA, Lago S (2000) J Chem Phys 113:7306–7316
54. Camaioni DM, Schwerdtfeger CA (2005) J Phys Chem A 109:10795–10797
55. Liptak MD, Shields GC (2001) Int J Quantum Chem 85:727–741
56. Barthelemy JF, Jost R, Sommer J (1978) Org Magn Reson 11:438–442
57. Kaur D, PreetKaur R, Kuhli R (2009) J Mol Struct (THEOCHEM) 913:90–96
58. Scott AP, Radom LJ (1996) J Phys Chem 100:16502–16513
59. Taft RW (1983) Prog Phys Org Chem 14:247–350
60. Breneman CM, Wiberg KB (1990) J Comput Chem 11:361–373
61. Haloui A, Haloui E work in progress
62. Barone V, Cossi M, Tomasi J (1997) J Chem Phys 107:3210–3221
63. Ginovska B, Camaioni DM, Dupuis M, Schwerdtfeger CA, Gil Q (2008) J Phys Chem A 112:10604–10613
64. Zimmermann T, Burda JV (2009) J Chem Phys 131(135101):1–12
65. Takano Y, Houk KN (2005) J Chem Theor Comput 1:70–77
66. Marenich VA, Cramer JC, Truhlar GD (2009) J Phys Chem B 113:6378–6396